

DESY SR 84-14
April 1984

X-RAY ABSORPTION NEAR EDGE STRUCTURE OF METAL HYDRIDES

by

B. Lengeler, R. Zeller

Inst. f. Festkörperforschung, Kernforschungsanlage Jülich

Eigentum der Property of	DESY	Bibliothek library
Zugriff Access	21. JUNI 1984	
Leihfrist Loan period:	7	days

ISSN 0723-7979

DESY behält sich alle Rechte für den Fall der Schutzrechtserteilung und für die wirtschaftliche Verwertung der in diesem Bericht enthaltenen Informationen vor.

DESY reserves all rights for commercial use of information included in this report, especially in case of filing application for or grant of patents.

To be sure that your preprints are promptly included in the
HIGH ENERGY PHYSICS INDEX ,
send them to the following address (if possible by air mail) :

DESY
Bibliothek
Notkestrasse 85
2 Hamburg 52
Germany

DESY SR 84-14
April 1984

ISSN 0723-7979

X-ray absorption near edge structure of metal hydrides

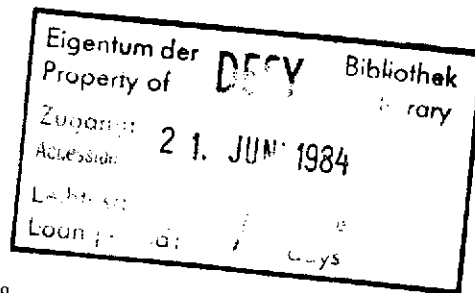
B. Lengeler and R. Zeller

Institut für Festkörperforschung, Kernforschungsanlage
Jülich, Postfach 1913, 5170 Jülich Germany

ABSTRACT

We have measured the X-ray absorption near edge structure (XANES) at K, L₁, L₂ and L₃ edges of Ti, V, Cr, Ni, Zr, Nb, La, Ce and Lu hydrides. The p-projected densities of empty states for Ni and NiH have been derived from band structure calculations which extend to 36 eV above the Fermi level. We show that the structure in the absorption edge of Ni hydride reflects the structure for the p-projected density of empty states.

submitted to J. of Less Common Metals



ISSN 0723-7979

1. Introduction

A major breakthrough in the understanding of the electronic structure of hydrogen in metals has been achieved by the band structure calculations of A.C. Switendick and later by many other groups /1-7/. The basic points emerging from these calculations are the following:

1. Among the electronic host states, those most strongly affected by the dissolved hydrogen have s-character at the hydrogen site.
2. Since the proton is a strong perturbation, electronic states can be shifted in energy by considerable amounts (up to 10 eV).
3. The dissolution of hydrogen is favored strongly if states which are empty in the host are shifted by hybridisation with hydrogen wavefunctions below the Fermi level.
4. In metal-hydrogen systems with more than one hydrogen per unit cell the H-H interaction can create new states below the Fermi level E_F .
5. If not enough new states are created and if not enough empty states are shifted below E_F the remaining electrons have to be accommodated at the Fermi level.

The band structure calculations are the best basis for explaining the various experimental results on hydrides obtained with very different techniques: Electronic specific heat, magnetic susceptibility and magnetization, nuclear magnetic resonance (see e.g. /1/), Mössbauer effect /8/, de Haas-van Alphen effect /9-10/ and

Compton scattering /11/ have all been used to study H in metals. Techniques which probe densities of occupied and empty electronic states such as photoemission /12/ and photoabsorption are especially interesting for testing band structure calculations.

In the present paper we present X-ray absorption measurements on Ti, V, Cr, Ni, Zr, Nb, La, Ce and Lu hydrides which were used to determine p- and d-projected densities of empty states. We have performed a band structure calculation for Ni and NiH from which the density of empty p-states was deduced. We will show that the structure in the K edge of nickel hydride basically reflects the structure in the empty p-states.

2. X-ray absorption near edge structure (XANES)

Figure 1 shows the principle of the technique /13/. When the energy E of a photon exceeds the binding energy E_0 of e.g. a 1s electron in Ni then a K absorption process can occur. Due to the conservation of angular momentum transitions are only allowed (in the dipole approximation) between electronic states with $|\Delta l| = 1$. This means that a 1s or 2s electron can only end up in empty p-states (K and L_1 absorption). Electrons from 2p states will end up mainly in d states (L_2 and L_3 edges). The XANES spectroscopy probes the empty, projected, local electronic densities of states $D_l(E)$. Müller et al /14/ have shown that the X-ray absorption coefficient μ can be written as

$$\mu(E) \sim m_l(E) D_l(E) \quad (1)$$

The transition matrix element $m_l(E)$ is weakly dependent on the energy. The structure in μ reflects basically the structure in $D_l(E)$. The first X-ray absorption measurements on hydrides were done with photons from X-ray tubes /15-16/. These measurements were hampered by the poor energy resolution which smears out the details in the structure of the edges and hence can lead to a wrong location of the Fermi level. With the advent of highly collimated, intense and tunable X-rays from storage rings the situation has improved considerably on the experimental side as will be shown.

3. Experimental details

The samples used in the present investigation were prepared from high purity metals by gas absorption ($TiH_{1.90 \pm 0.01}$, $VD_{0.72 \pm 0.01}$, $ZrH_{1.98 \pm 0.01}$, $NbH_{0.93 \pm 0.01}$, $LaH_{2.00 \pm 0.02}$, $LaH_{2.96 \pm 0.02}$, $CeH_{1.92 \pm 0.02}$, $CeH_{2.65 \pm 0.02}$, $LuH_{1.96 \pm 0.05}$, $LuH_{3.0 \pm 0.05}$) or by electrolysis ($CrH_{1.00 \pm 0.01}$ and $NiH_{0.85 \pm 0.01}$). Ni foils of 5 μm thickness were charged at room temperature in 1 n sulfuric acid (50 mA/cm², Pt anode) for 24 hours. A 5 μm thick film of chromium hydride was deposited on 2.5 μm Cu foils in a solution of CrO_3 and water according to a method described by Knödler /17/. The Ni and Cr hydrides were stored in liquid nitrogen in order to prevent the hydrogen from escaping from the samples. The hydrogen concentration in these alloys was determined by heat extraction. The lattice constants (at 25 °C) of hexagonal CrH were found by X-ray diffraction to be $a = 2.719 \text{ \AA}$ and $c = 4.430 \text{ \AA}$. The hydrogen concentration in the other hydrides was determined from

the amount of absorbed gas. These hydrides were ground in an agate mortar in a glove box and stored under purified argon. Immediately before the measurements powder layers of appropriate thickness were packed between two Kapton foils. In addition to the hydrides metal foils of high purity were analysed.

All measurements were done in transmission at the beam line ROEMO at the Hamburger Synchrotronstrahlungslabor. The photon intensities were measured by ionisation chambers. For photon energies E below 10 keV a Si(111) double crystal monochromator was used with an energy resolution of 1.5 eV FWHM at 10 keV. For energies above 10 keV a Si(220) cut was used (energy resolution 1.2 eV at 10 keV). The first crystal of the monochromator was cut asymmetrically with an angle of 5° between the surface and the reflecting planes. For the second crystal this angle was zero. This allows rejection of the harmonics without loss of intensity. The amount of harmonics was continuously monitored by means of a NaI scintillation counter. The electron energy in the storage ring DORIS was 3.7 GeV. Small shifts in the beam position and beam direction are especially embarrassing in XANES studies since they can produce changes in the photon energy (at the same monochromator setting) by 0.5 eV or more. In order to distinguish this effect from real shifts in the edges e.g. between Ni and Ni hydride we have measured at the same time with the edge of Ni hydride the edge of a pure Ni between the second and a third ionisation chamber. This arrangement of three ionisation chambers in a row with two samples measured at the same time allows one to locate the absorption edges relative to one another with an accuracy of ± 0.1 eV.

4. Experimental results

The figures 2-3 show the K edges of Ti, V, Cr, Ni, Zr and Nb in the pure metals and in the hydrides listed above. The jumps at the edge have been normalized to one. The pure metals show increasing structure in the edges with decreasing atomic number Z . An especially strong peak is visible in the edge of metallic Ti. As a rule, the K edges of the hydrides have less pronounced structures. This is also true for the L_1 edges of La, Ce and Lu hydrides (figure 3,4). The L_3 edges of the rare earths and their hydrides are characterized by strong white lines which reflect the high density of empty d -states just above the Fermi level. The normalized L_2 and L_3 edges are identical. There are only minor differences in the L_1 , L_2 and L_3 edges of the di- and trihydrides of the rare earths (figures 3,4).

5. Band structure calculations for Ni and NiH

We have performed band structure calculations for Ni and NiH using self-consistent potentials obtained by the local density approximation /18/ to the density functional theory. The lattice parameters used for the fcc Ni and NiH were 3.47 \AA and 3.724 \AA , respectively. The value for the NiH was taken from our EXAFS analysis on $\text{NiH}_{0.85}$. The value for Ni is a theoretical one, determined by the self-consistent potential of Moruzzi et al /20/ which we use in our calculation. The experimental lattice parameter for Ni at 77 K is 3.514 \AA /19/.

The KKR method used in the present calculation for Ni is described in reference 20. The expansion of the wavefunctions in spherical harmonics is truncated at $l = 4$. Figure 5 shows the result of the calculation for Ni. In the case of NiH a similar procedure to that adopted for Ni was not possible. We have constructed a self-consistent potential by the linear band structure method of augmented spherical waves /5,21/. Since this linear method does not yield accurate unoccupied bands at higher energies, the potential was brought into muffin-tin form and the bands were calculated by the APW method (figure 5). The wavefunctions at the symmetry points Γ , X, W, L and U = K were analysed according to their l -character at the Ni sites and at the octahedral sites in Ni and NiH. The predominant character is marked in figure 5 on the left hand side of a symmetry point for the Ni site and on the right hand side of a symmetry point for the octahedral site (which is empty in Ni and occupied by hydrogen in NiH). A comparison of the two band structures shows that the main changes occur for those states which have s-character at the octahedral site and these are lowered considerably in energy by the attractive potential of the hydrogen. Some states which are empty in Ni (like L_2') are lowered below the Fermi level in the hydride. They accommodate part of the additional electrons. The rest of these is accommodated in the lowest free states thus moving up the Fermi level above the d-bands. The results obtained in the present calculation are in qualitative agreement with those by Switendick /1/ and Gupta and Burger /5/, but ours extend to higher energies which is of interest for the comparison with the XANES.

In order to do this comparison we have calculated the p-projected local density of empty states at the Ni sites using the tetrahedron method for the Brillouin zone integration with 6144 tetrahedrons for Ni and 756 tetrahedrons for NiH. The results are shown in figure 6. Also shown in this figure is the slowly varying matrix element $m_1(E)$ for NiH which differs only slightly from that for pure Ni. The main effect of the hydrogen is to lower the peak positions from 3, 8, 17 and 25 eV in pure Ni to 1, 5, 12 and 19 eV in NiH. The first three of these peaks are related to the bands at X_4 , W_3 and X_5 , U_4 , L_2 , which have mainly p character at the Ni site. The peaks at 25 eV in Ni and 19 eV in NiH are caused by band extrema not visible in figure 5 /22/. In the lower part of figure 6b we show the measured K-absorption edge for NiH_{0.85} and the calculated product $m_l(E) \cdot D_l(E)$ for NiH which has been convoluted with a Lorentzian. The width of the Lorentzian is energy dependent. It varies between 2.6 eV at E_0 and 6.2 eV at 40 eV above E_0 and takes into account the core hole lifetime, the final state lifetime /14/ and the experimental resolution (quoted above). The theoretical energy scale has been expanded by 5 %. The fair agreement between theory and experiment shows that the structure in the XANES is mainly due to the structure in $D_l(E)$. The need for rescaling the energy axis was also observed by other groups /23/ who justified it with the influence of the core hole. It is not clear if this is also the reason in the present case.

Although the projected density of states of NiH is far from constant and the broadened curve shows no arctangent behavior the calculation locates the Fermi level at the first inflection point of the edge (figure 6). This is not true, however, for pure Ni because the peak at 3 eV in $D_1(E)$ leads to a displacement by 0.75 eV of the first inflection point to higher energies. The calculation, on the other hand, gives an alignment of the K-edges of Ni and NiH as in figure 6 (same value E_0 for Ni and NiH_{0.85}). This means that the energy difference between the 1s state and the Fermi level is the same in Ni and NiH_{0.85} to within ± 0.1 eV.

6. Conclusions

1. We have presented experimental results of K, L_1 , L_2 and L_3 X-ray absorption edges for a number of metal hydrides. The K and L_1 edges of the hydrides have less structure in the edges than the corresponding pure metals.
2. A band structure calculation for Ni and NiH extending up to 36 eV above E_F has been performed. The hydrogen lowers host states with s-character at the octahedral interstices especially strongly.
3. The main structures in the absorption edges reflect the structures in the projected densities of empty states ($D_1(E)$ in the case of the K edges in Ni and NiH). Additional effects such as the rescaling of the energy axis by 5 % between the measured XANES and the absorption coefficient deduced from the projected densities of state are not yet understood.

Acknowledgements

The authors would like to thank Mr. H.J. Bierfeld for preparing the gas loaded hydrides and Drs. B.M. Klein and W.E. Pickett for introducing them into the use of their APW program.

REFERENCES

1. A.C. Switendick in "Hydrogen in Metals I" ed. G. Alefeld and J. Völkl, Topics in Appl. Phys. 28, 101 (1978), Springer Verlag.
2. D.A. Papaconstantopoulos, B.M. Klein, E.N. Economu and L.L. Boyer, Phys. Rev. B17, 141 (1978).
3. C.D. Gelatt, H. Ehrenreich and J.A. Weiss, Phys. Rev. B17, 1940 (1978).
4. D.A. Papaconstantopoulos, B.M. Klein, J.S. Faulkner and L.L. Boyer, Phys. Rev. B18, 2784 (1978).
5. M. Gupta and J.P. Burger, J. Phys. F10, 2649 (1980).
6. D.K. Misemer and B.N. Harmon, Phys. Rev. B26, 5634 (1982).
7. D.J. Peterman, D.K. Misemer, J.H. Weaver, D.T. Peterson, Phys. Rev. B27, 799 (1983).
8. F.E. Wagner and G. Wortmann, in ref. 1., p. 131.
9. W.R. Wampler and B. Lengeler, Phys. Rev. B15, 4614 (1977).
10. R. Griessen and L.M. Huisman, in "Electronic Structure and Properties of Hydrogen in Metals", P. Jena and C.B. Satterthwaite (eds.), Plenum Press (1983), p. 235.
11. R. Lässer and B. Lengeler, Phys. Rev. B18, 637 (1978).
12. J.H. Weaver, D.J. Peterman and D.T. Peterson, in ref. 10, p. 207.
13. A. Bianconi, L. Incoccia and S. Stipcich (eds.) "EXAFS and Near Edge Structure" Springer Series in Chemical Physics 27 (1983).
14. J.E. Müller, O. Jepsen and J.W. Wilkins, Sol. State Comm. 42, 365 (1982).

15. O. Brümmer, G. Dräger and H. Baum, Z. Naturforschg 18a, 1102 (1963).
 16. A. Faessler and R. Schmid, Z. Phys. 190, 10 (1966).
 17. A. Knödler, Metalloberfläche 17, 161 (1963).
 18. L. Hedin and B.I. Lundquist, J. Phys. C4, 2064 (1971).
 19. J. Donohue, The Structures of the Elements, J. Wiley & Sons (1974).
 20. V.L. Moruzzi, J.F. Janak and A.R. Williams, Calculated Electronic Properties of Metals (Pergamon, New York, 1978).
 21. A.R. Williams, J. Kübler and C.D. Gelatt, Jr., Phys. Rev. B19, 6094 (1979).
 22. F. Szmulowicz and D.M. Pease, Phys. Rev. B17, 3341 (1978).
 23. G. Materlik, J.E. Müller and J. Wilkins, Phys. Rev. Lett. 50, 267 (1983).
- L.A. Grunes, Phys. Rev. B27, 2111 (1983).

Figure Captions

Fig. 1: X-ray absorption in the near edge region.

Fig. 2: XANES at the K edges of Ti, $\text{TiH}_{1.90}$, V, $\text{VD}_{0.72}$, Cr
CrH, Ni and $\text{NiH}_{0.85}$.

Fig. 3: XANES at the K edges of Zr, $\text{ZrH}_{1.98}$, Nb, $\text{NbH}_{0.93}$ and
at the L_1 and L_3 edges of γ -Ce, $\text{CeH}_{1.92}$ and $\text{CeH}_{2.65}$.

Fig. 4: XANES at the L_1 and L_3 edges of La, $\text{LaH}_{2.0}$, $\text{LaH}_{2.96}$
 $\text{LuH}_{1.96}$ and $\text{LuH}_{3.0}$.

Fig. 5: Band structure of Ni and NiH. The letters s, p, d, f
give the predominant wave character at the Ni site (left
from symmetry point) and at the octahedral site (right
from symmetry point).

Fig. 6: a) p-projected densities of states $D_1(E)$ for Ni (dashed)
and NiH (full line) and matrix element $m_1(E)$ for NiH.
b) Comparison of the measured XANES (crosses) of $\text{NiH}_{0.85}$
with the absorption coefficient calculated from the
band structure calculation (full line).

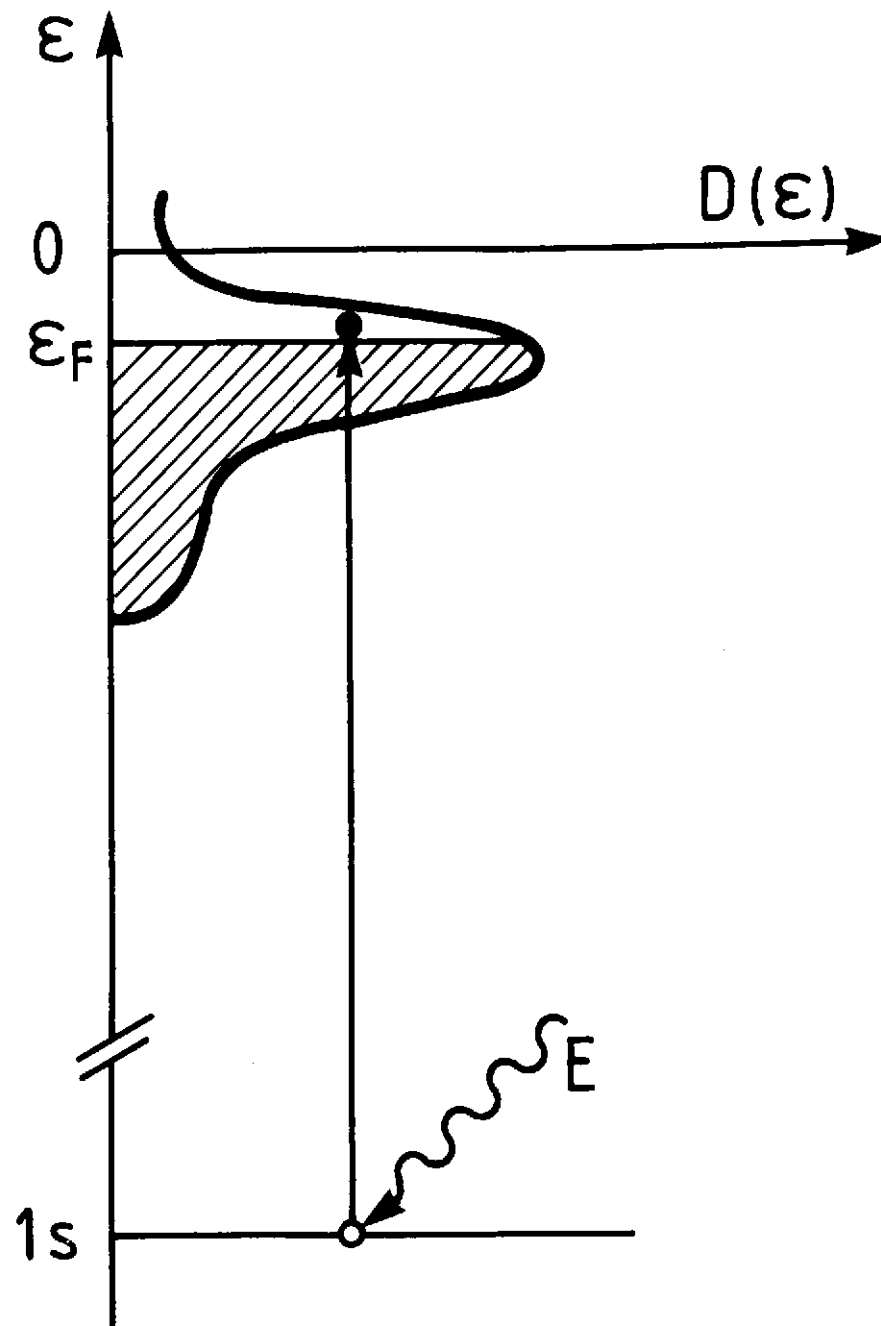


Fig. 1

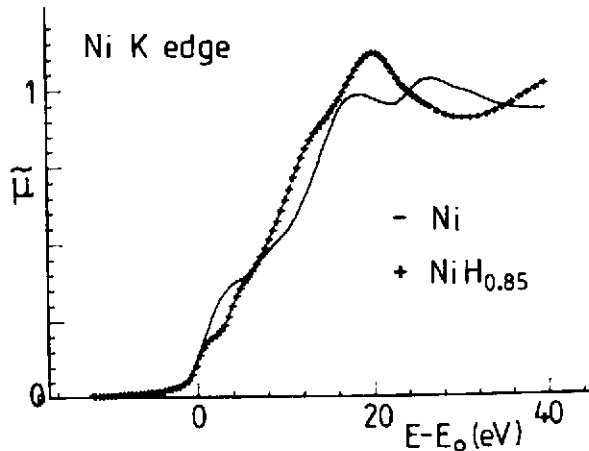
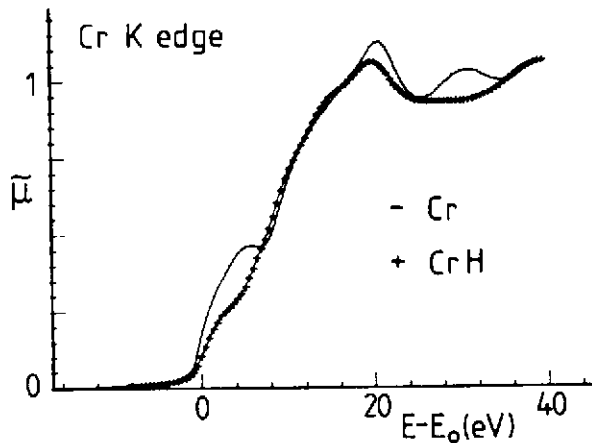
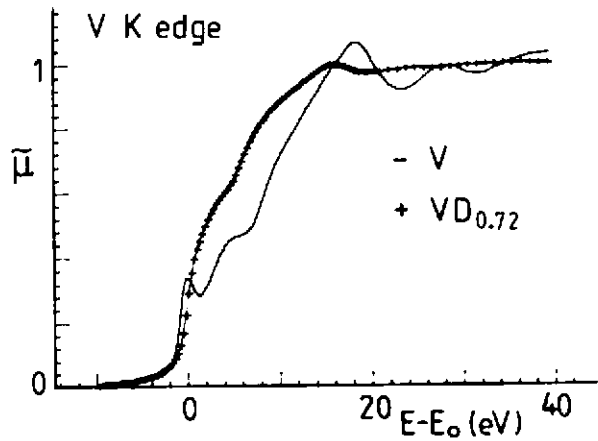
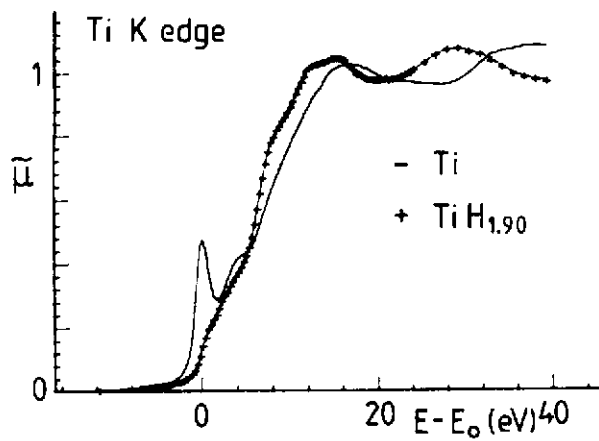


Fig. 2

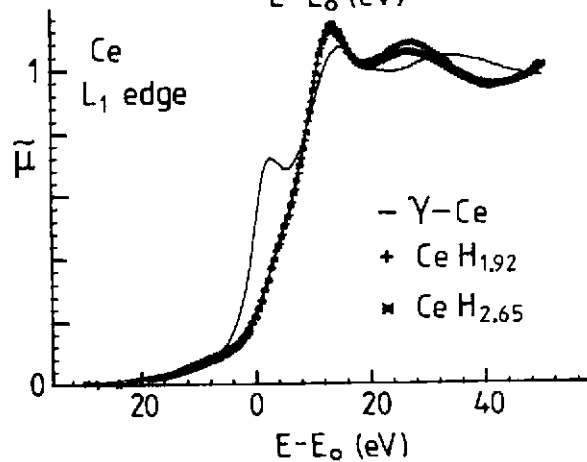
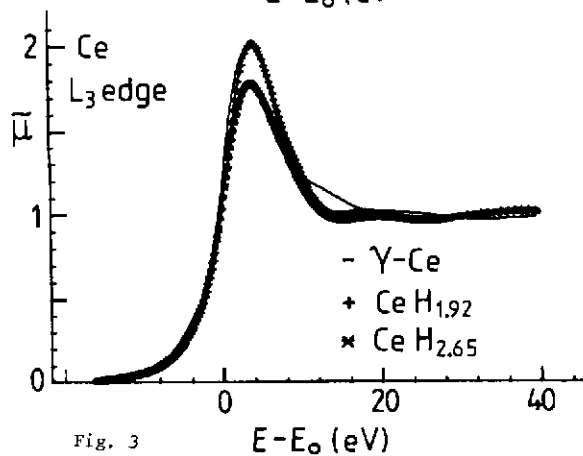
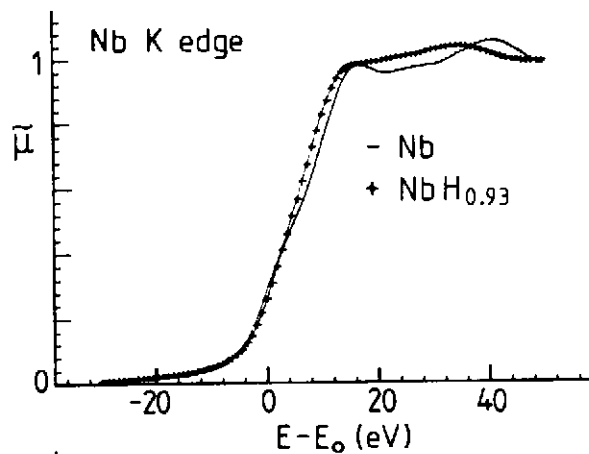
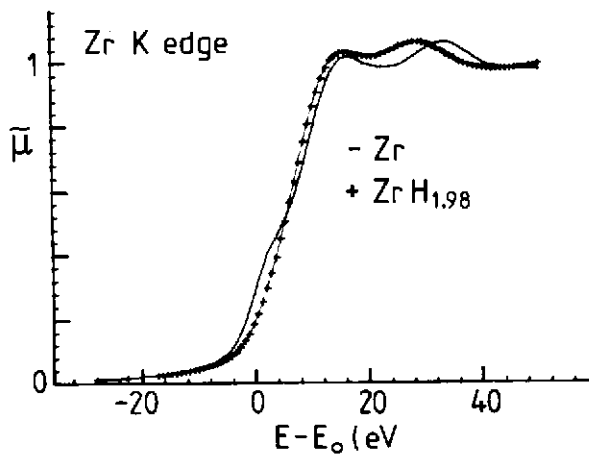


Fig. 3

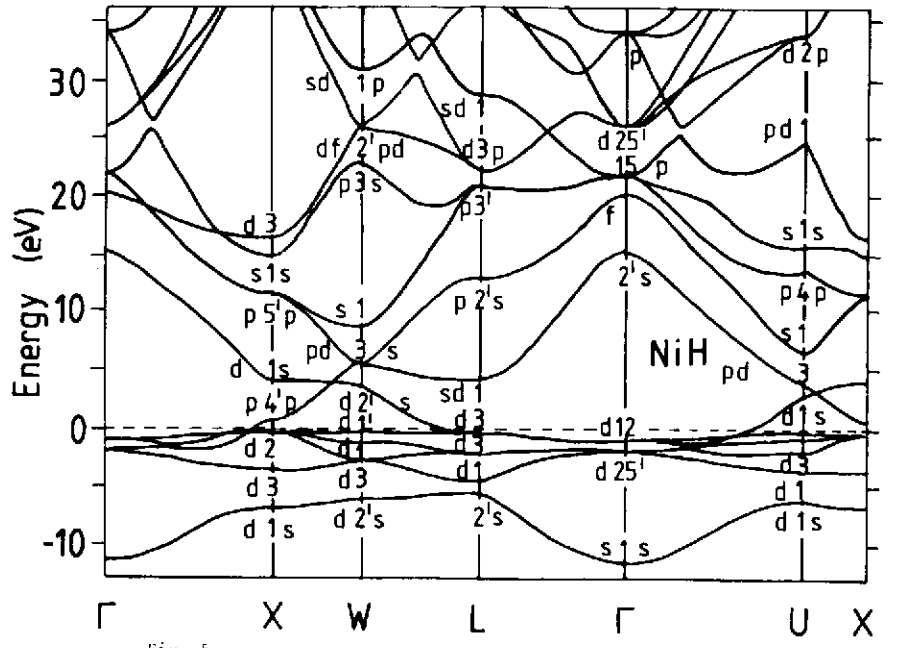
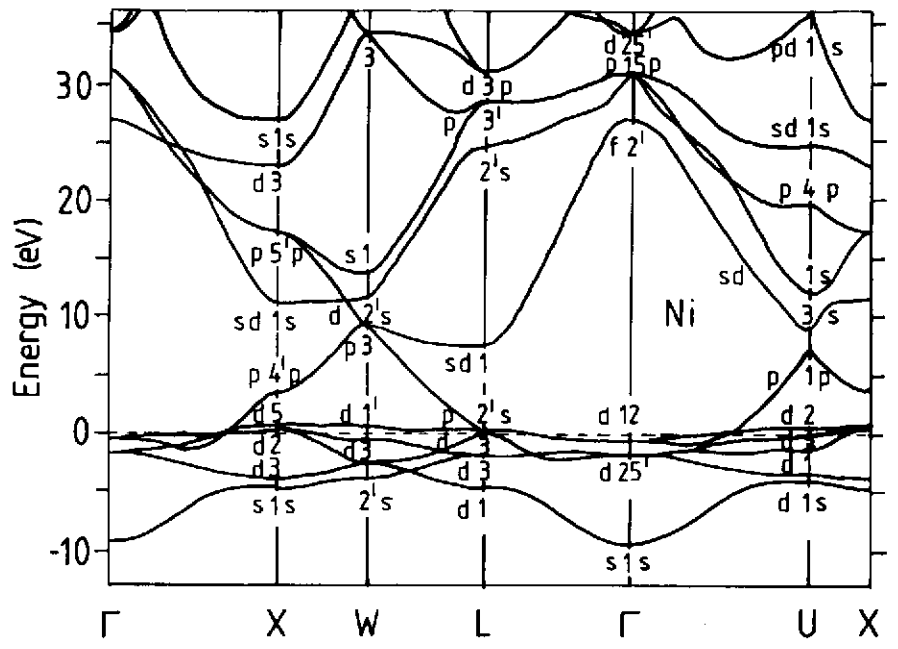
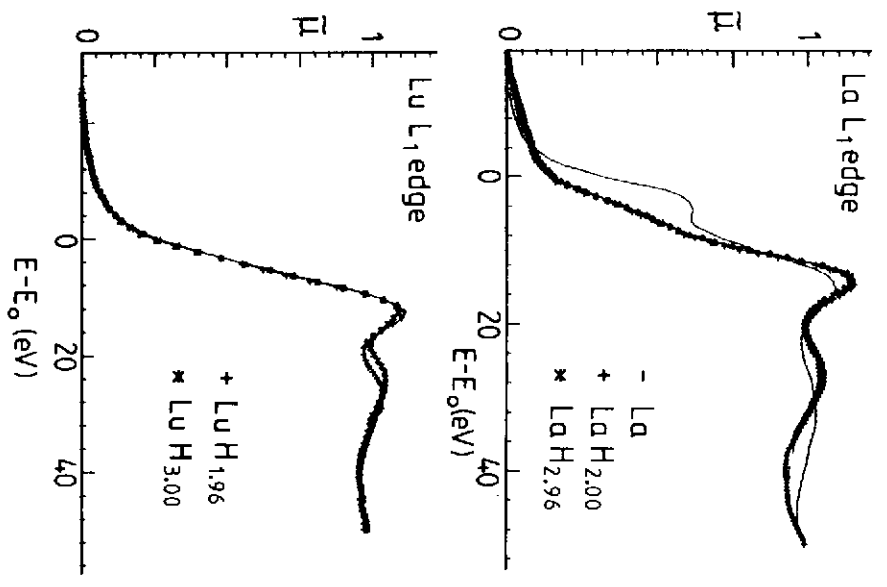
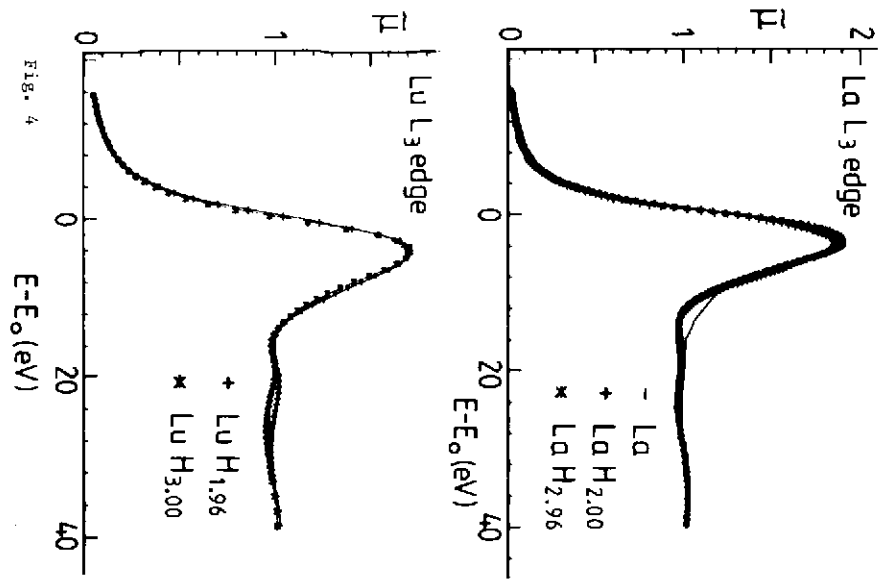


Fig. 5

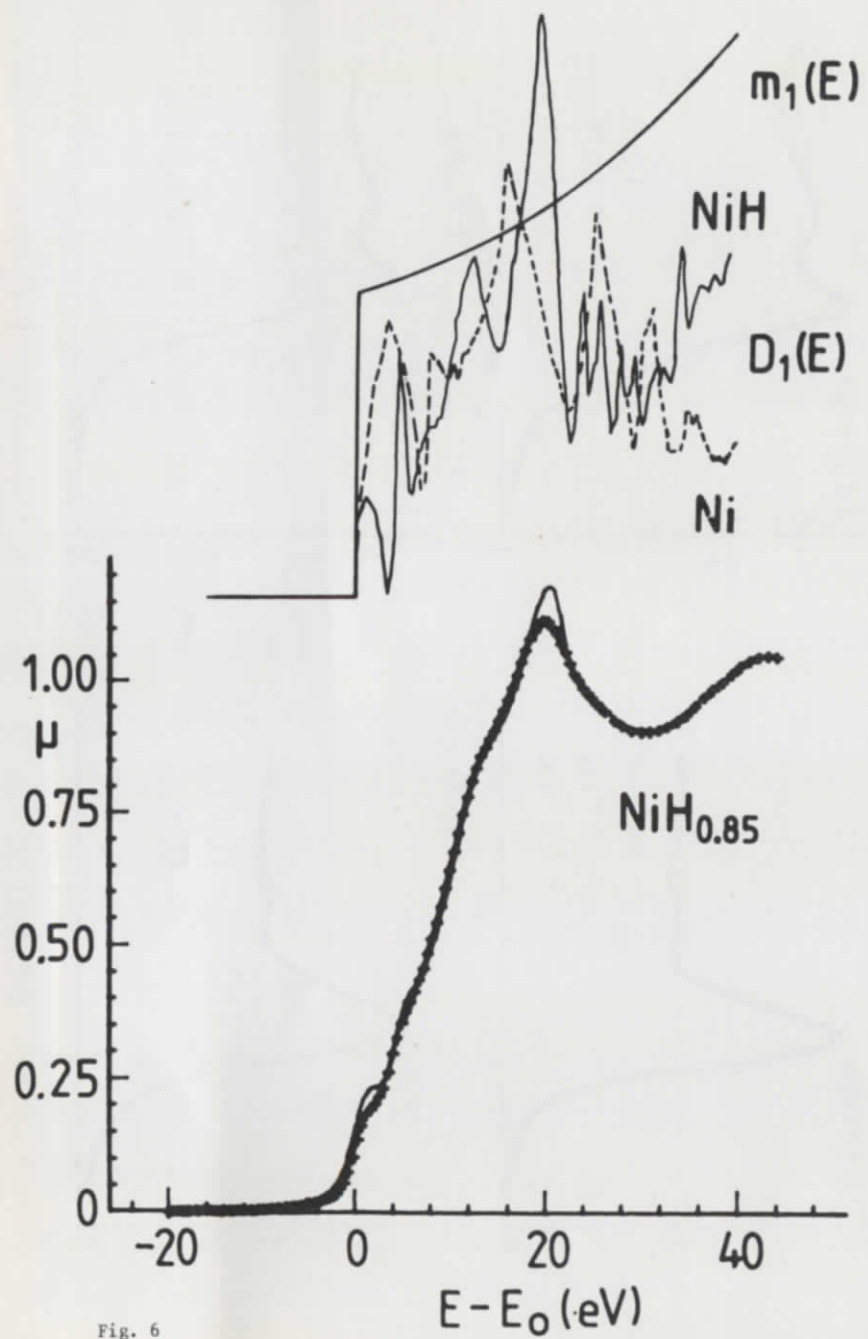


Fig. 6